

# Cavity Sound Resonance and Mass Transfer in Aerated Agitated Tanks

Linda S. De More,  
William F. Pafford, and  
Gary B. Tatterson

Mechanical Engineering Department  
Texas A&M University  
College Station, TX 77843

Gas dispersion occurs from gas cavities which are formed behind rotating impeller blades in aerated, agitated tanks. Sound is generated in this process which can be used to characterize the process when detected using a hydrophone. However, a hydrophone is a pressure transducer which detects pressure waves and does not exclusively detect sound if other pressure changes are present in the flow.

Pseudosounds are pressure changes which are not sound, i.e., which do not propagate elastically through a medium. Examples of pseudosounds include changes in dynamic pressure and hydrostatic head, pressure fluctuations due to turbulence and viscosity changes in laminar non-Newtonian fluid flow. Pseudosounds can be easily mistaken for actual sound and their characterization is necessary before studies of actual sound can be properly accomplished.

The discharge velocity from behind an impeller blade is much greater than the discharge velocity from in front of the blade (e.g., Mujumdar et al., 1970). These changes in the discharge velocity cause changes in dynamic pressure, which a stationary hydrophone detects as a pseudosound at the blade passing frequency in pressure spectra; the relationship being:

$$\Delta P = \frac{1}{2} \rho (\Delta V_D^2). \quad (1)$$

For gas/liquid discharge from the impeller, the density of the flow as well as the discharge velocity change between the front and back of the blade giving rise to pseudosound.

In gas/liquid discharge flows, the dynamic pressure change does not necessarily remain constant from blade passage to blade passage. Specifically, the 3-3 structure (Warmoeskerken et al., 1981) has an alternating nature in its discharge flow. The discharge from a clinging cavity alternates with the discharge from a large cavity. In this case, the pseudosounds occur at one half the blade passing frequency in the pressure spectra of the hydrophone. Harmonic series are also present in the pressure spectra because of the time signal waveform of the hydrophone.

Pressure spectra of hydrophone may also contain pseudosounds generated because of changes in hydrostatic head; a simple model being:

$$\Delta P = \Delta(\rho_D g H). \quad (2)$$

Gas bubbles produce sound by volume oscillations in bubble size (Strasberg, 1956) and have a natural resonant frequency which is related to bubble size by Eq. 3:

$$f_o = \frac{(3\gamma P_o / \rho)^{1/2}}{2\pi R_o}. \quad (3)$$

Bubbles at their natural resonance frequency generate very high sound pressure levels (Strasberg, 1953). The product,  $f_o R_o$ , can also be considered a peak resonance velocity. It is suspected that gas cavities resonate at a natural frequency since they are essentially gas pockets. The resonance may be due to a frequency associated with bubble entry and bubble detachment.

## Separation between Sound and Pseudosounds

The hydrophone signal contains local flow information because of dynamic pressure changes, distant flow information, perhaps because of changes in hydrostatic pressure, e.g., surface waves, and sound information from local and distant sound sources, such as from bubble and cavity oscillations. However, separation of the different sound and pseudosound sources can be accomplished by analysis of the amplitude and frequency of the hydrophone signal.

Cavity sounds in the pressure spectra can be identified by performing studies to identify the natural resonance frequency of the cavities and by changing the nature of the cavity structures.

## Objectives

Time signals of a stationary hydrophone near the impeller were obtained to confirm the dynamic pressure mechanism for

the production of pseudosound as described above. Pressure spectra in a cavity resonance study, obtained using a hydrophone mounted on the impeller, were investigated for the possible appearance of a natural frequency or a peak resonance velocity for the cavity structures residing on the impeller blades.

## Experimental Study

The experimental equipment used in this work has been described elsewhere: Sutter et al. (1987), Ursy et al. (1987), and Hsi et al. (1985). The College Station tap water used in the study was electrolytic ( $\text{Na}^+$  212 mg/L,  $\text{Cl}^-$  54 mg/L).

Hydrophone time signals were obtained in time records 0.4 seconds in length for impeller rotational speeds of 3.08, 3.67, 4.58, 5.0 and  $5.9 \text{ s}^{-1}$  and at gassing rates of  $0$ ,  $6.6 \times 10^{-3}$ ,  $9.4 \times 10^{-3}$ ,  $11.3 \times 10^{-3}$ , and  $13.7 \times 10^{-3} \text{ m}^3/\text{s}$ . For these records, the hydrophone was held stationary at a fixed position approximately 13 mm from the passing blade and in the center of the lower half of the blade. The rotation of a magnetic chip, mounted on the rotating shaft above on impeller blade, was detected and displayed simultaneously with the hydrophone time signal.

For the cavity resonance study, sound spectra measurements were taken with the hydrophone mounted behind the blade in the cavity structures. A slip ring was used to transfer the hydrophone signal from the rotating shaft. A search was conducted to identify the natural resonance of the cavity structures in the spectra. Impeller rotational speeds studies were from  $3.33$  to  $4 \text{ s}^{-1}$ , and gassing rates were  $4.7 \times 10^{-3}$ ,  $7.1 \times 10^{-3}$ ,  $9.4 \times 10^{-3}$  and  $11.8 \times 10^{-3} \text{ m}^3/\text{s}$ . Studies were also performed with the hydrophone located in the same orientation but with the impeller blade removed.

Based on correlations provided by Nienow et al. (1985), Taterson and Morrison (1987), and Smith and Warmoeskerken (1985), most of the conditions selected for study were in the 3-3 gas cavity structure regime. Gassed power data as a function of impeller rotational speed and gassing rate for our tank configuration were available in Nienow et al. (1977).

## Hydrophone Time Signal Study

The ungassed and gassed hydrophone time signals are given in Figure 1 and show the periodicity of the impeller discharge

flow at the blade passing frequency under both conditions. The various amplitudes of the signals are not constant with time which indicates that the liquid pumping from individual impeller blades was not constant. For the hydrophone time signals obtained at rotational speeds of  $5.0$  and  $5.9 \text{ s}^{-1}$  and a gassing rate of  $6.6 \times 10^{-3} \text{ m}^3/\text{s}$ , the cavities systems residing on the impeller blades were fairly undefined. For the remaining gassing rates and impeller rotational speeds, the 3-3 structure resided on the six blade disk style turbine and the hydrophone time signals were typical of the 3-3 structure.

The time signal waveform of the 3-3 structure, Figure 2, is associated with the alternating clinging/large 3-3 cavity structure. At point A, a large negative voltage exists which is the response to a discharge from a large cavity passing over the hydrophone. At point B, liquid pumping, which is occurring between large and clinging cavities, is present. At point C, another negative voltage exists but is not as large as that of the large cavity. This represents the passing of a clinging cavity over the hydrophone. Again, at point D, liquid pumping is occurring. At point E, the hydrophone is again detecting a large cavity.

## Cavity Resonance Study

The cavity resonance spectra are shown in Figure 3. Using the resonance frequencies shown in the figure and Eq. 3, a physical size estimate for the resonance is 15 mm in radius or about one third to fourth of the blade width of the impeller. The resonant peaks in Figure 3 occur at ten times the blade passing frequency or 60 times the impeller rotational speed which is within the typical range of shear rates for the disk style impeller. In the single phase study by Metzner et al. (1961), average shear rate was 11.5 times the impeller rotational speed for the disk style turbine. Maximum shear rates for the disk style turbine have also been estimated to be ten times the average shear rates of the impeller (Metzner et al., 1960; van't Riet and Smith, 1975; Calabrese et al., 1987) or 100 times the impeller rotational speed.

The spectra in Figure 3 show groups of peaks at impeller rotational speeds from  $3.33$  to  $4 \text{ s}^{-1}$  at gassing rates of  $4.7 \times 10^{-3}$ ,  $7.1 \times 10^{-3}$ ,  $9.4 \times 10^{-3}$  and  $11.8 \times 10^{-3} \text{ m}^3/\text{s}$ . Outside of these ranges of impeller rotational speed and gassing rates, the groups of peaks disappeared. When these peaks are fully developed (i.e.,  $N = 3.66 \text{ s}^{-1}$  in Figure 3), three sets of three peaks each are present. This 3-3 pattern did not change significantly with

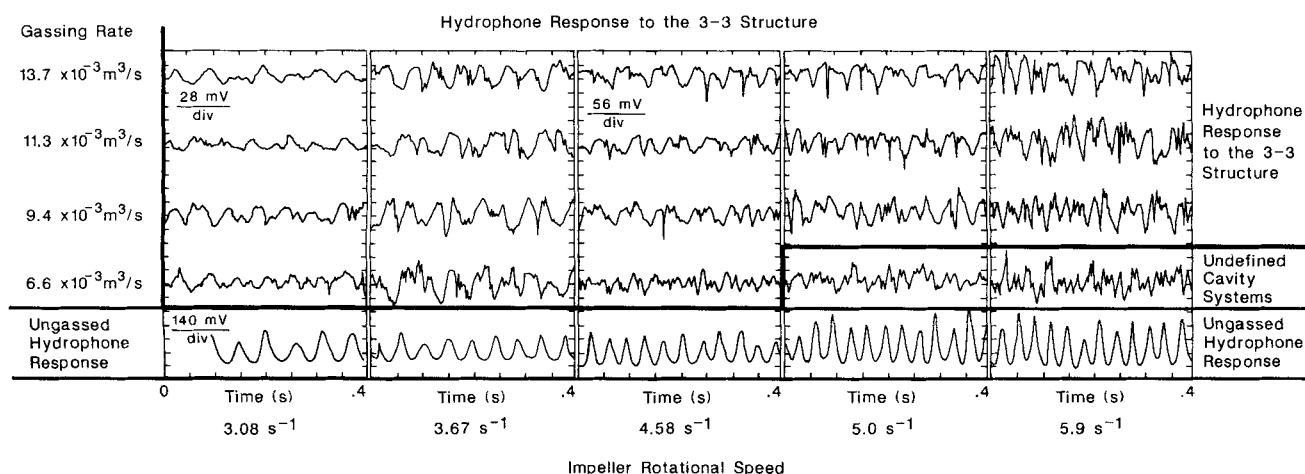


Figure 1. Hydrophone response for various impeller rotational speeds and gassing rates.

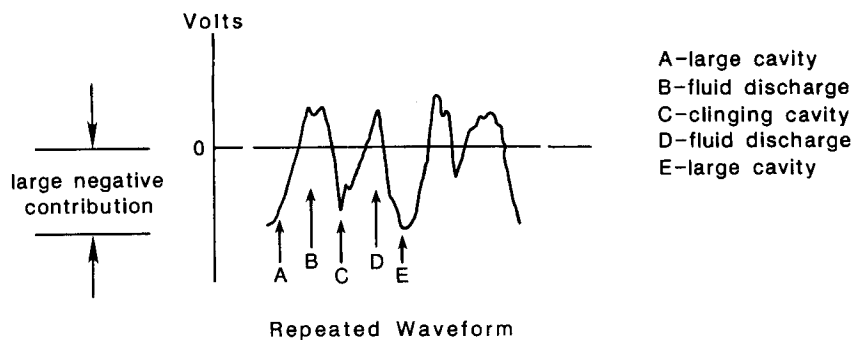


Figure 2. Hydrophone with respect to cavities and impeller blade for the repeated waveform.

increasing gassing rate, however, significant changes occur when the rotational speed was varied. The dynamic pressure pseudosound was not present in the spectra since the hydrophone was mounted on the blade.

Figure 4 shows a plot of the area under the resonance peaks in Figure 3 vs. the aeration number,  $N_Q$  or  $Q/ND^3$ . From these data, the aeration numbers at maximum resonance,  $N_{Qm}$ , were obtained as a function of gassing rate as:

$$N_{Qm} = 9.65 \text{ s/m}^3 Q. \quad (4)$$

Cancelling the gassing flow rate from both sides and rearranging:

$$ND^3 = 0.104 \text{ m}^3/\text{s}. \quad (5)$$

Since the impeller diameter was fixed at 0.3048 m in this work, the impeller rotational speed at maximum resonance is fixed at  $3.67 \text{ s}^{-1}$ . The impeller tip speed at maximum resonance is 3.51 m/s which corresponds remarkably well with the peak reso-

nance velocity, 3.39 m/s, obtained from Eq. 3 for conditions of this work.

To show further that the resonance peaks of Figure 3 were associated with the cavity structures, spectra were obtained under the same conditions with the blade removed. The resulting spectra were significantly different from those shown in Figure 3. Multiple peaks and resonance were again observed in the spectra, however, there was no set observable 3-3 pattern to the peak arrangement. The peaks occurred over a larger frequency range than did the peaks in the spectra shown in Figure 3.

Bubble sounds were not distinctly recognized in the pressure spectra obtained in this study. Surface waves under nongassing conditions were observed as pseudosounds. Under gas sparging conditions and impeller rotational speeds in this study, surface waves were not a significant pseudosound source.

### Cavity Peak Resonance and Mass Transfer

Smith et al. (1977) presented detailed data of  $k_L a/V_s^{0.4}$  for the transfer of oxygen from air into electrolytic water versus gassed power per volume,  $P_g/V$ , for standard geometries, i.e.,  $D/T =$

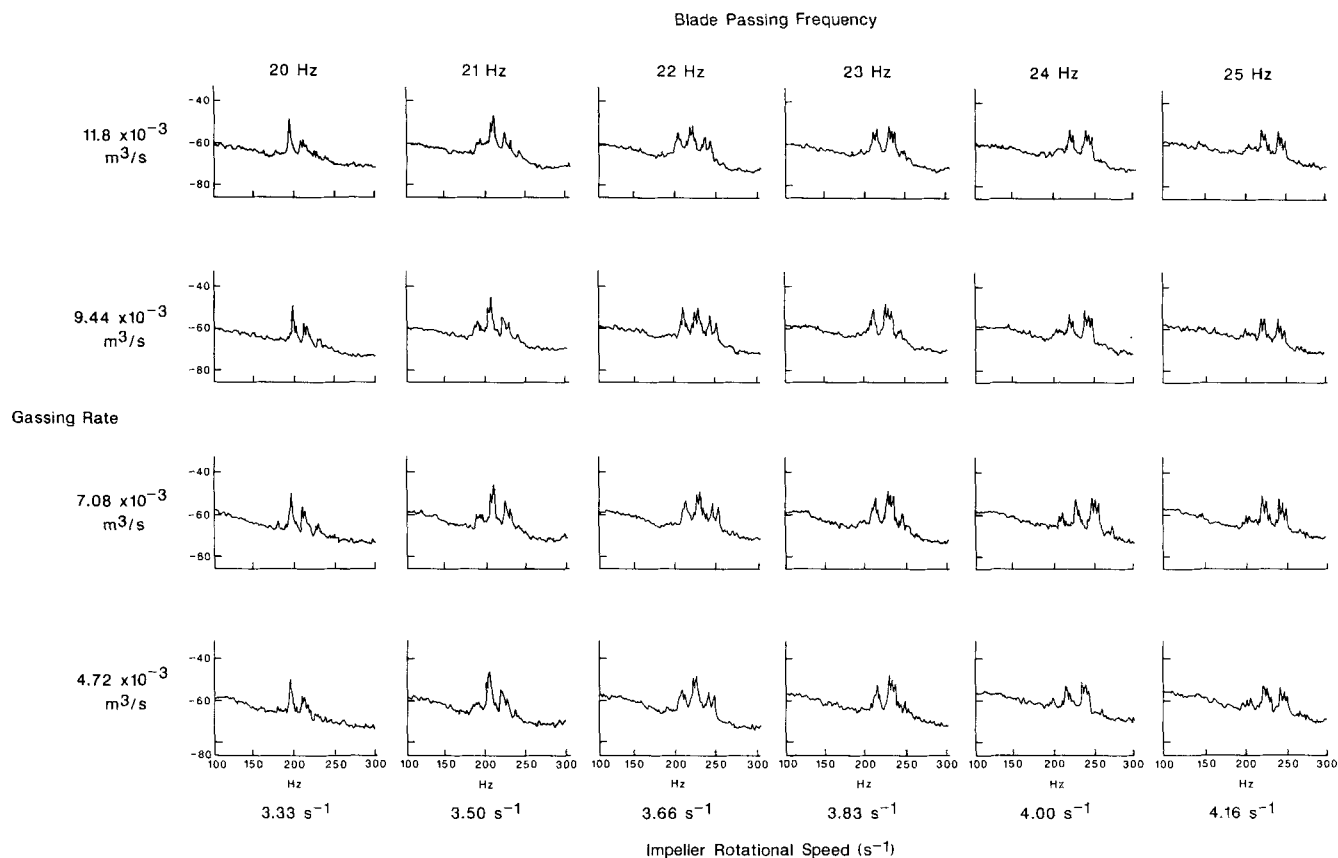


**Figure 3. Cavity peak resonance spectra as a function of gassing rate and impeller rotational speed: ordinate span – 40 to – 60 dB; abscissa span 100 to 300 Hz.**

0.33 and 0.5, and tanks sizes,  $T = 0.61, 0.91$  and  $1.83$  m for the disk style turbine. Some of the data have been reproduced in Figure 5. In certain cases, as noted by Smith et al.,  $k_L a / V_s^{0.4}$  data actually decreased as gassed power per volume increased, directly contradicting typical literature correlations for the mass transfer coefficient (e.g., Yagi and Yoshida, 1975; van't Riet, 1979). This occurred for gassed power per volume above  $700$   $W/m^3$  and impeller tip speeds which ranged from  $3.9$  to  $5.2$  m/s for different tank diameters from  $0.61$  to  $1.83$  m and  $D/T$  ratios of  $0.33$  and  $0.5$  as shown in Figure 5.

Figure 5 also shows integral peak areas for cavity resonance of Figure 3 vs. specific shaft gas power per volume and impeller tip velocities. As can be observed in the figure, the behavior of

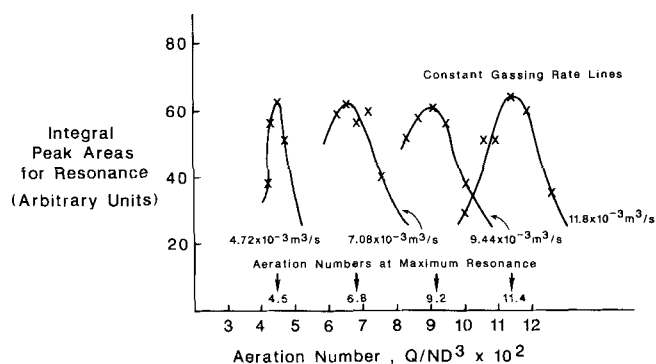


**Figure 4. Integral peak areas vs. aeration number.**

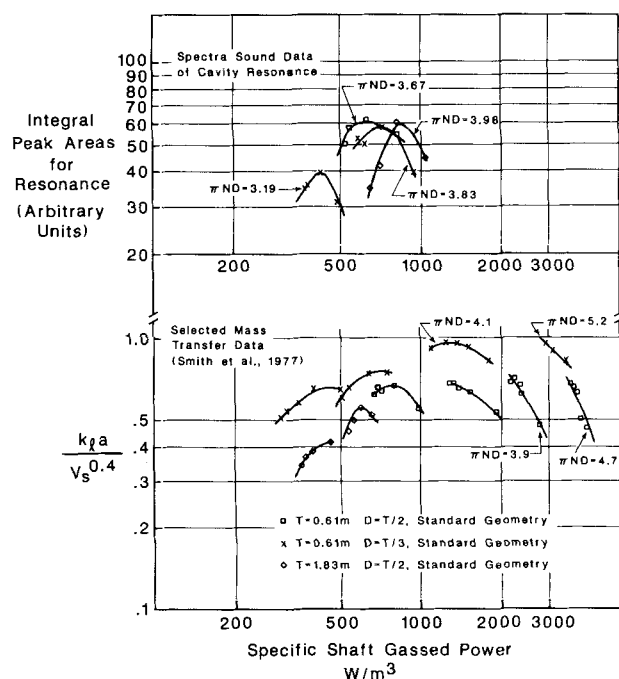


**Figure 5.  $k_L a / V_s^{0.4}$  data and integral peak areas as a function of specific shaft gassed power and impeller tip speed.**

the integral peak areas of the resonance and the  $k_1a/V_s^{0.4}$  data is similar. The maximum cavity resonance observed in this work for electrolytic water occurred in the gassed power input range between 450 to 720 W/m<sup>3</sup> and at a fixed impeller tip speed of 3.51 m/s for a tank diameter of 0.9 m and a  $D/T$  ratio of 0.33.

The  $k_1a$  data, reported by Smith et al. (1977), contained 12 maximums in  $k_1a$  for various operating conditions and tank sizes. However, an average of the 12 impeller tip velocities for the maximums was found to be 3.56 m/s which is very close to the peak resonance velocity, 3.51 m/s, of the cavities.

The results permit the following interpretation with regard to mass transfer optimization and the mass transfer coefficient. For optimization, from the correspondence shown in Figure 5, cavity resonance follows the mass transfer optimization parameter,  $k_1a/V_s^{0.4}$ . For the mass transfer coefficient, as indicated by  $k_1a$  data reported by Smith et al. (1977), maximums in  $k_1a$  occur at the impeller tip velocity equal to the peak resonance velocity of the cavities. If changes in  $k_1$  are assumed negligible, maximum cavity peak resonance corresponds with maximum production of interfacial area,  $a$ , for electrolytic systems and the disk style impeller reaches a choked flow condition.

## Acknowledgments

LSD wishes to thank the Program for Supplemental Funding for Support of Undergraduate Women Engineering Research Assistants of the National Science Foundation, Grant No. CBT-8514127, for her support. WFP and GBT acknowledge support from the National Science Foundation, Grant No. CBT-8619756.

## Notation

$a$  = interfacial area  
 $D$  = impeller diameter  
 $f$  = frequency  
 $f_o$  = natural resonant frequency  
 $g$  = acceleration of gravity  
 $H$  = hydrostatic head  
 $k_1a$  = mass transfer coefficient  
 $N$  = impeller rotational speed, revolutions/time  
 $N_Q$  = aeration number,  $Q/ND^3$   
 $N_{Qm}$  = aeration number,  $Q/ND^3$ , at maximum resonance  
 $P$  = dynamic pressure  
 $P_g$  = gassed power input  
 $P_o$  = static or ambient pressure  
 $Q$  = gassing rate  
 $R_o$  = bubble or cavity radius  
 $T$  = tank diameter  
 $V$  = tank volume  
 $V_D$  = discharge velocity  
 $V_s$  = superficial gas velocity  
 $\rho$  = liquid density

$\rho_D$  = local dispersion density  
 $\gamma$  = ratio of specific heats

## Literature Cited

- Calabrese, R. V., N. A. Bryner, B. J. Sadoff, and C. M. Stoots, "The Velocity Field Relative to a Stirred Tank Turbine Blade," Engineering Foundation Conference on Mixing: Mixing XI, New England College, Henniker, NH (Aug. 2-7, 1987).
- Hsi, R., M. Tay, D. Bukur, G. L. Morrison, and G. B. Tatterson, "Sound Spectra of Gas Dispersion in an Agitated Tank," *Chem. Eng. J.*, **31**, 153 (1985).
- Metzner, A. B., and J. S. Taylor, "Flow Patterns in Agitated Vessels," *AIChE J.* **6**(1), 109, (Jan., 1960).
- Metzner, A. B., R. H. Feehs, H. L. Ramos, R. E. Otto, and J. D. Tuthill, "Agitation of Viscous Newtonian and Non-Newtonian Fluids," *AIChE J.*, **7**(1), 3 (1961).
- Mujumdar, A. S., B. Huang, D. Wolf, M. E. Weber, and W. J. M. Douglas, "Turbulence Parameters in a Stirred Tank," *Can. J. Chem. Eng.*, **48**, 475 (1970).
- Nienow, A. W., D. J. Wisdom, and J. C. Middleton, "The Effect of Scale and Geometry on Flooding, Recirculation, and Power in Gassed Stirred Vessels," *Proc. Eur. Conf. on Mixing*, St. John's College, Cambridge, England, Paper F1 (1977).
- Nienow, A. W., M. Konno, and W. Bujalski, "Studies on Three-Phase Mixing: A Review and Recent Results," *Proc. Eur. Conf. on Mixing*, Wurzburg, Germany, Paper 2 (1985).
- Smith, J. M., K. van't Riet, and J. C. Middleton, "Scale-Up of Agitated Gas-Liquid Reactors for Mass Transfer," *Proc. Eur. Conf. on Mixing*, St John's College, Cambridge, England, Paper F4 (1977).
- Smith, J. M., and M. M. C. G. Warmoeskerken, "The Dispersion of Gases in Liquids with Turbines," *Proc. Eur. Conf. on Mixing*, Wurzburg, Germany, Paper 13 (1985).
- Strasberg, M., "Gas Bubbles as Sources of Sound in Liquids," *J. Acoust. Soc. of Amer.*, **28**(1), 20 (1956).
- Sutter, T. A., G. L. Morrison, and G. B. Tatterson, "Sound Spectra in an Aerated Agitated Tank," *AIChE J.*, **33**, 529 (1987).
- Tatterson, G. B., and G. L. Morrison, "Effect of Tank to Impeller Diameter Ratio on Flooding Transition for Disc Turbines," *AIChE J.*, **33**, 1751 (1987).
- Ursy, W. R., G. L. Morrison, and G. B. Tatterson, "On the Interrelationship between Mass Transfer and Sound Spectra in an Aerated Agitated Tank," *Chem. Eng. Sci.*, **42**, 1856 (1987).
- van't Riet, K., and J. M. Smith, "The Trailing Vortex System Produced by Rushton Turbine Agitators," *Chem. Eng. Sci.*, **30**, 1093 (1975).
- van't Riet, K., "Review of Measuring Methods and Results in Nonviscous Gas-Liquid Mass Transfer in Stirred Vessels," *I&EC: Proc. Des. Dev.*, **18**(3), 357 (1979).
- Warmoeskerken, M. M. C. G., J. Feijen, and J. M. Smith, "Hydrodynamics and Power Consumption in Stirred Gas-Liquid Dispersions," *ICHEME. Sym. Ser.*, No. 64, J1 (1981).
- Yagi, H., and F. Yoshida, "Gas Absorption by Newtonian and Non-Newtonian Fluids in Sparged Agitated Vessels," *I&EC: Proc. Des. Dev.*, **14**(4), 488 (1975).

Manuscript received Sept. 15, 1987, and revision received May 16, 1988.